An Investigation of Hydrogen Bonding in Benzoxazine Dimers by Fast Magic-Angle Spinning and Double-Quantum ^{1}H NMR Spectroscopy

Ingo Schnell,[†] Steven P. Brown,[†] Hong Yee Low,[‡] Hatsuo Ishida,[‡] and Hans Wolfgang Spiess*,[†]

Contribution from the Max-Planck-Institut für Polymerforschung, Postfach 3148, D-55021 Mainz, Germany, and Department of Macromolecular Science, Case Western Reserve University, Cleveland, Ohio 44106

Received August 3, 1998. Revised Manuscript Received September 9, 1998

Abstract: A combination of solid-state ^{1}H NMR techniques, namely MAS, CRAMPS, and DQ MAS spectroscopy, is used to investigate the hydrogen-bonding properties of a range of alkyl-substituted benzoxazine dimers in the solid state. These dimers are of interest because they serve as model compounds for a class of recently synthesized polymers, the polybenzoxazines, whose unusual properties, in particular a near-zero shrinkage or volumetric expansion upon curing, have been rationalized in terms of favorable hydrogen-bonding interactions. The enhanced resolution achievable at the only recently available very-fast MAS rotation frequency of 35 kHz coupled with the sensitivity of the ^{1}H chemical shift to the hydrogen-bonding arrangement means that much useful information can be obtained by simple MAS alone. In addition, spectra obtained by using a recently introduced CRAMPS approach, suitable for fast MAS and requiring no special experimental setup, are presented. Comparing the methyl- and ethyl- (and *n*-propyl-) substituted dimers, the significant shifts to low field of the chemical shifts of the hydrogen-bonded protons, as well as the observation of a second aromatic peak only in the latter case, suggest different packing arrangements for the different dimers. On the basis of the additional information about proton proximities provided by the presence or absence of peaks in two-dimensional DQ MAS spectra, it is shown that, while for the methyl dimer, as previously proposed, pairs of hydrogen-bonded dimers are present, for the ethyl and *n*-propyl dimer, an alternative linear arrangement of hydrogen-bonded dimers predominates.

Introduction

Information about hydrogen bonding in solids[1] can be obtained by a variety of methods, in particular X-ray and neutron diffraction, and NMR[2] and IR[3] spectroscopy. In principle, NMR spectroscopy has the advantage of allowing the direct probing of the hydrogen-bonded protons themselves. However, ^{1}H NMR spectroscopy of rigid solids is complicated by the homonuclear proton−proton dipolar interaction;[4−6] this leads to substantial homogeneous broadening of the resonances, typically of the order of 50 kHz, such that chemical shift information is usually obscured.

To overcome this problem, solid-state NMR investigations of hydrogen bonding have employed multiple-pulse methods, the first example being the WHH-4 sequence developed by Waugh, Huber, and Haeberlen,[7] to remove the homonuclear dipolar broadening, such that the ^{1}H chemical shifts can be resolved. An alternative approach for investigating hydrogen bonds is the determination of ^{2}H quadrupolar coupling constants, e.g. by nuclear quadrupole resonance.[8] For a general hydrogen bond O−H···O, clear correlations have been established between both the so-measured ^{1}H chemical shifts and ^{2}H quadrupolar coupling constants and the O···H and O···O distances[9−11]; the latter, which have been determined by the diffraction techniques, are a direct measure of the strength of the hydrogen bond. Additionally, interesting information about hydrogen-bonded structures has been obtained by NMR experiments which utilize cross polarization from ^{1}H to a "dilute" nucleus, e.g. ^{13}C or ^{29}Si.[12,13]

Hydrogen bonds are known to play an important role in determining the properties of a range of materials.[14−16] Re-

* To whom correspondence should be addressed.
[†] Max-Planck-Institut für Polymerforschung.
[‡] Case Western Reserve University.

(1) Hamilton, W. C.; Ibers, J. A. *Hydrogen Bonding in Solids*; Benjamin: New York, 1968.
(2) Becker, E. D. *Encyclopedia of Nuclear Magnetic Resonance*; Wiley: Chichester, 1996; Vol. 4, p 2409.
(3) McQuade, D. T.; McKay, S. L.; Powell, D. R.; Gellman, S. H. *J. Am. Chem. Soc.* **1997**, *119*, 8528.
(4) Abragam, A. *The Principles of Nuclear Magnetism*; Clarendon: Oxford, 1961.
(5) Mehring, M. *Principles of High-Resolution NMR in Solids*; Springer: Berlin, 1983.
(6) Schmidt-Rohr, K.; Spiess, H. W. *Multidimensional Solid State NMR and Polymers*; Academic Press: New York, 1994.
(7) Waugh J. S.; Huber L. M.; Haeberlen, U. *Phys. Rev. Lett.* **1968**, *20*, 180.
(8) Hunt, M. J.; Mackay, A. L. *J. Magn. Reson.* **1974**, *15*, 402.
(9) Berglund, B.; Vaughan, R. W. *J. Chem. Phys.* **1980**, *73*, 2037.
(10) Jeffrey, G. A.; Yeon, Y. *Acta Crystallogr.* **1986**, *B42*, 410.
(11) Harris, R. K.; Jackson, P.; Merwin, L. H.; Say, B. J.; Hagele, G. *J. Chem. Soc., Faraday Trans.* **1988**, *84*, 3649.
(12) Chuang, I.-S.; Maciel, G. *J. Am. Chem. Soc.* **1996**, *118*, 401.
(13) Gu, Z.; Ridenour, C. F.; Bronnimann, C. E.; Iwashita, T.; McDermott, A. *J. Am. Chem. Soc.* **1996**, *118*, 822.
(14) Sijbesma, R. P.; Beijer, F. H.; Brunsveld, L.; Folmer, B. J. B.; Hirschberg, J. H. K. K.; Lange, R. F. M.; Lowe, J. K. L.; Meijer, E. W. *Science* **1997**, *278*, 1601.
(15) Brunet, P.; Simard, M.; Wuest, J. D. *J. Am. Chem. Soc.* **1997**, *119*, 2737.
(16) Castellano, R. K.; Rebek, J., Jr. *J. Am. Chem. Soc.* **1998**, *120*, 3657.

10.1021/ja982766t CCC: $15.00
Published on Web 10/28/1998

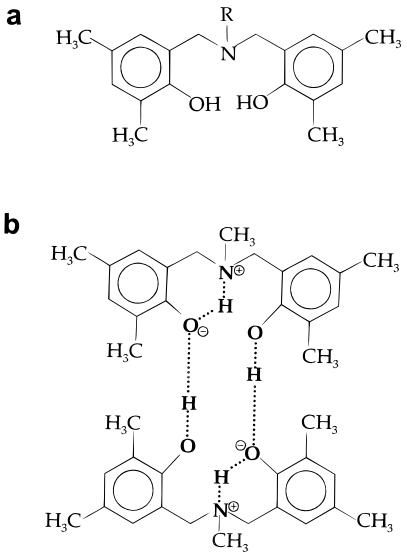

Figure 1. (a) The structure of a generic benzoxazine dimer. In this study, dimers with four different alkyl substituents, R = methyl, ethyl, *n*-propyl, or *n*-butyl, were investigated. (b) A schematic representation of a pair of benzoxazine dimers linked by an extended hydrogen-bonding arrangement, as proposed by Dunkers *et al.*[23] for the methyl dimer.

cently, the synthesis and characterization of a new class of phenolic materials, the polybenzoxazines, has been described by Ishida and co-workers.[17−20] These polybenzoxazine resins were found to have a number of unusual, but commercially favorable, properties, in particular a near-zero shrinkage or volumetric expansion upon curing (polymerization) as well as low water absorption. In addition, the resins have high glass-transition temperatures even though they have been shown to have low cross-link densities. Explanations for these properties have been hypothesized in terms of favorable hydrogen-bonding interactions.[21]

To better investigate these interactions, a series of model benzoxazine dimers—*N*,*N*-bis(3,5-dimethyl-2-hydroxybenzyl) "R" amine, where "R" = methyl, ethyl, *n*-propyl, or *n*-butyl—were synthesized.[22] The chemical structure of a generic dimer is shown in Figure 1a. To date, the hydrogen bonding in these dimers has been investigated by IR spectroscopy, X-ray diffraction, and molecular modeling.[23] On the basis of this work, the presence of pairs of dimers linked by an extended hydrogen-bonded arrangement involving both intermolecular O−H···O and intramolecular N−H···O hydrogen bonds, as represented in Figure 1b, has been proposed for the methyl dimer. The purpose of this paper is to show, as a specific example, that recently developed fast magic-angle spinning (MAS) and double-quantum (DQ) NMR methods outlined below can provide further information, which is both unique and complementary to that achievable by other approaches, on the hydrogen bonding in such samples.

In powdered solids, to obtain a high-resolution spectrum, both the homogeneous and inhomogeneous broadenings associated with the homonuclear dipolar interaction and the chemical shift anisotropy (CSA), respectively, have to be removed. This can be achieved by combining the multiple-pulse sequences with conventional MAS in the so-called combined rotation and multiple pulse spectroscopy (CRAMPS) method.[24−26] However, this technique is experimentally demanding to implement, requiring the use of specially prepared spherical samples to minimize B_1 inhomogeneity and the careful setting of pulse flip angles and phases.

Over the past decade, much progress has been made in the area of fast MAS,[27] and probes capable of a rotation frequency, ν_R, of 35 kHz are now commercially available. In this paper, it is shown that the resolution afforded by such a fast ν_R means that important information about hydrogen bonding can now be obtained by MAS alone. Additionally, the enhanced resolution achievable by rotor-synchronized CRAMPS methods, applicable at high ν_R, is demonstrated. CRAMPS is normally performed at a slow ν_R, typically 2−3 kHz, such that the sample is "quasi-static" during the application of the multiple-pulse sequence, so as to avoid destructive interference. In this paper, results obtained by both a recently presented rotor-synchronized CRAMPS approach, which combines a semi-windowless multiple-pulse sequence and MAS at a ν_R of up to 15 kHz,[28] and a new modification which uses a standard WHH-4 sequence at 35 kHz are presented. These methods have the advantage over conventional CRAMPS of delivering comparable resolution enhancement without requiring the complicated and time-consuming extended setup procedure.

In solution-state ^{1}H NMR, much additional information about both through-bond and through-space proton distances can be obtained by extending the NMR experiment to a second dimension.[29] In the solid state, it has recently been shown that DQ MAS spectroscopy[30−34] can, in principle, yield similar information about the through-space proximity of dipolar-coupled nuclei. However, the ability to harness the information inherent to such a two-dimensional DQ MAS spectrum is very dependent on the resolution in both frequency dimensions.[35] In this paper, it is shown that the dramatic increase in resolution achievable at a ν_R of 35 kHz means that important structural information can now be obtained from ^{1}H DQ MAS spectra.

Experimental Details

The benzoxazine dimers were synthesized as described by Dunkers and Ishida.[22] ^{1}H MAS NMR experiments were performed on a Bruker ASX 500 spectrometer at a ^{1}H Larmor frequency of 500.1 MHz, using a double-resonance MAS probe supporting rotors of outer diameter 2.5 mm with a spinning frequency of up to 35 kHz. At these very fast spinning frequencies, the additional heating effect caused by air friction becomes significant. By using the ^{119}Sn resonance of $Sm_2Sn_2O_7$ as a chemical shift thermometer,[36] the correction term relative to the bearing

(17) Ning, X.; Ishida, H. *J. Polym. Sci. Chem. Ed.* **1994**, *32*, 1121.
(18) Ishida, H.; Allen, D. J. *J. Polym. Sci. Phys. Ed.* **1996**, *34*, 1019.
(19) Shen, S. B.; Ishida. H. *Polym. Compos.* **1996**, *17*, 5.
(20) Ishida, H.; Low, H. Y. *Macromolecules* **1997**, *30*, 1099.
(21) Wirasate, S.; Dhumrongvaraporn, S.; Allen, D. J.; Ishida, H. *J. Appl. Polym. Sci.* Accepted for publication.
(22) Dunkers, J.; Ishida, H. *Spectrochim. Acta* **1995**, *51A*, 855.
(23) Dunkers, J.; Zarate, E. A.; Ishida, H. *J. Phys. Chem.* **1996**, *100*, 13514.
(24) Gerstein, B. C.; Pemberton, R. G.; Wilson, R. C.; Ryan L. M. *J. Chem. Phys.* **1977**, *66*, 361.
(25) Scheler, G.; Haubenreisser, U.; Rosenberger, H. *J. Magn. Reson.* **1981**, *44*, 134.
(26) Maciel, G. E.; Bronnimann, C. E.; Hawkins, B. L. *Adv. Magn. Reson.* **1990**, *14*, 125.
(27) Jakobsen, H. J. *Encyclopedia of Nuclear Magnetic Resonance*; Wiley: Chichester, 1996; Vol. 1, p 398.
(28) Hafner, S.; Spiess, H. W. *Solid State Nucl. Magn. Reson.* **1997**, *8*, 17.
(29) Ernst, R. R.; Bodenhausen, G.; Wokaun, A. *Principles of Nuclear Magnetic Resonance in One and Two Dimensions*; Clarendon: Oxford, 1987.
(30) Geen, H.; Titman, J. J.; Gottwald, J.; Spiess, H. W. *Chem. Phys. Lett.* **1994**, *227*, 79.
(31) Sommer, W.; Gottwald, J.; Demco, D. E.; Spiess, H. W. *J. Magn. Reson.* **1995**, *A113*, 131.
(32) Gottwald, J.; Demco, D. E.; Graf, R.; Spiess, H. W. *Chem. Phys. Lett.* **1995**, *243*, 314.
(33) Feike, M.; Graf, R.; Schnell, I.; Jäger, C.; Spiess, H. W. *J. Am. Chem. Soc.* **1996**, *118*, 9631.

gas temperature was determined, in a separate experiment, to range from 37 K at room temperature (294 K) to 25 K at a bearing gas temperature of 338 K. All stated temperatures have been corrected by this procedure. If not explicitly stated, an experiment was performed with the bearing gas at room temperature. For all samples, the 90° pulse length was 2.0 μs, and a recycle delay of 10 s was used. For one-dimensional MAS experiments, 16 transients were averaged. In addition, a solution-state ^{1}H NMR spectrum of the ethyl dimer dissolved in deuterated chloroform was recorded on a Bruker DPX 250 spectrometer at a ^{1}H Larmor frequency of 250.1 MHz.

CRAMPS spectra were obtained for the ethyl dimer, using the WHH-4 multiple-pulse sequence[7] in either a semi-windowless form[28] (1 μs$-P_x-P_{-y}-$2 μs$-P_y-P_{-x}-$ 1 μs, where P_ϕ denotes a 90° pulse of phase ϕ) at 13 kHz or in its standard form (6.15 μs$-P_x-$5.15 μs$-P_{-y}-$12.3 μs$-P_y-$5.15 μs$-P_{-x}-$6.15 μs) at 35 kHz, with 16 and 256 co-added transients, respectively. The cycle time, t_c, in the two cases equalled 12.0 and 42.9 μs, corresponding to 6 and 2/3 multiple-pulse cycles per rotor period. Data points were acquired, in quadrature-free mode, in the window between the P_{-y} and P_y pulses in the middle of each cycle. In both cases, the RF irradiation frequency was placed low field of the amine resonances. No special setup procedure or sample preparation methods were used in addition to those normally undertaken for standard MAS experiments.

DQ MAS experiments were performed with one cycle of the Back-to-Back (BABA) sequence[31] ($P_x-\tau-P_{-x}-P_y-\tau-P_{-y}$, where τ equals $\tau_R/2$ minus the pulse durations, with τ_R denoting a rotor period) for the excitation ($p = 0 \rightarrow p = \pm 2$, where p is the coherence order[29]) and reconversion ($p = \pm 2 \rightarrow p = 0$) of double-quantum coherences (DQCs). A final 90° pulse was used to create transverse magnetization, with the duration of the $p = 0$ "z-filter" period set equal to one rotor period. The total phase cycle[37] used consisted of 16 steps with 4 steps to select $p = \pm 2$ after the excitation sequence and four steps to select $p = 0 \rightarrow p = -1$. For each of 32 increments of t_1, 16 transients (consisting of 64 complex points) were averaged. Sign discrimination was restored in the F_1 dimension by the TPPI[38] method of incrementing the phase of the excitation pulses by 45°. The increments in both t_1 and t_2 were set equal to one rotor period such that spinning sidebands were removed in both frequency dimensions. In this way, the experimental time was reduced to only 85 min compared to 20 h for a spectrum with the minimum F_1 spectral width of 250 kHz necessary to avoid the folding-in of F_1 spinning sidebands. This, however, had the disadvantage that the baseline distortions of the strong alkyl peaks could not be corrected for, leading to small (maximum intensity 10%) negative intensity in the top left and bottom right of each spectra. In the contour plots, therefore, only positive contours are shown, with the bottom contour corresponding to 3% of the maximum intensity and subsequent contours corresponding to a multiplicative increment of 1.3.

One-Dimensional NMR Spectra

Ethyl Dimer. Figure 2 shows one-dimensional ^{1}H NMR spectra of the ethyl dimer for a range of physical states, namely (a) a simple MAS spectrum at 35 kHz and CRAMPS spectra at ν_R of (b) 13 and (c) 35 kHz of the rigid solid, (d) a simple MAS spectrum at 35 kHz of the melt at $T = 363$ K, and, for comparison, (e) a solution-state spectrum of the dimer dissolved in deuterated chloroform. The frequencies and intensities of the resolved resonances and their assignments for these spectra are given in Table 1. (It should be noted that the intensities of the overlapping resonance lines in Figure 2a were obtained by a fitting routine, while the distorted line shapes in the CRAMPS spectra meant that here such a fitting routine was unsuccessful.)

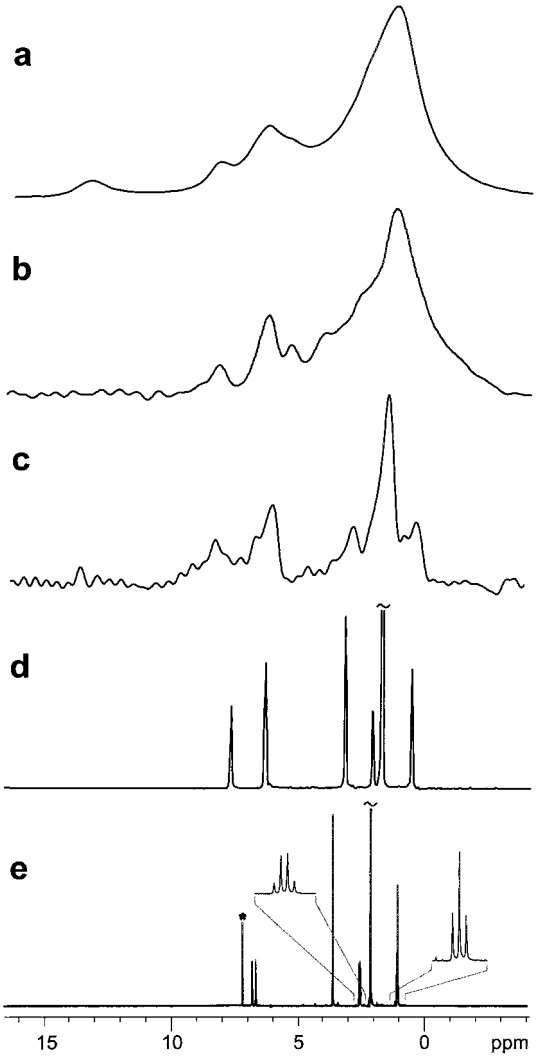

Figure 2. One-dimensional ^{1}H NMR spectra of the ethyl dimer for a range of physical states, namely (a−c) the solid, (d) the melt at a temperature of 363 K, and (e) dissolved in deuterated chloroform. Spectra (a) and (d) were recorded under MAS at 35 kHz, while (b) and (c) are CRAMPS spectra recorded with use of (b) a semi-windowless WHH-4 sequence at 13 kHz or (c) a standard WHH-4 sequence at 35 kHz. No weighting function was applied to the CRAMPS spectra. In spectra (d) and (e), the peaks corresponding to the *Ar*-CH_3 protons have been slightly truncated. The asterisk in spectrum (e) indicates the signal due to residual $CHCl_3$.

For the solution-state spectrum (Figure 2e), the assignment of the peaks is straightforward, since the methyl and methylene protons of the ethyl chain give rise to a familiar 1:2:1 triplet at 1.08 ppm and a 1:3:3:1 quartet at 2.56 ppm, respectively. (The peak marked with an asterisk corresponds to residual $CHCl_3$.) No peak is observed for the hydroxyl protons due to fast exchange, and hence the relative intensities of the other lines have been scaled appropriately such that the results are consistent with those for the solid and melt.

Figures 2a and 2d correspond to the two end-points of an investigation into the effect of temperature on the MAS spectrum, namely the rigid solid and the melt, respectively. Comparing Figures 2d and 2e and the assignment information in Table 1, it is evident that there is an approximately constant frequency shift of about 0.5 ppm between the corresponding peaks in the two spectra. Such frequency shifts between a molten and dissolved state have been observed before.[39] Additionally, an important difference is the appearance of a

(34) Graf, R.; Demco, D. E.; Gottwald, J.; Hafner, S.; Spiess, H. W. *J. Chem. Phys.* **1997**, *106*, 885.
(35) Schnell, I.; Lupulescu, A.; Hafner, S.; Demco, D. E.; Spiess, H. W. *J. Magn. Reson.* **1998**, *133*, 61.
(36) Grimmer, A.-R.; Kretschmer, A.; Cajipe, V. B. *Magn. Reson. Chem.* **1997**, *35*, 86.
(37) Bodenhausen, G.; Kogler, H.; Ernst, R. R. *J. Magn. Reson.* **1984**, *58*, 370.
(38) Marion, D.; Wüthrich, K. *Biochem. Biophys. Res. Commun.* **1983**, *113*, 967.

Table 1. Positions and Intensities of Resonances in the MAS Spectra of the Ethyl Dimer (Figure 2)

	expected		solution (Figure 2e)		melt (Figure 2d)		CRAMPS, 35 kHz	CRAMPS, 13 kHz	MAS, 35 kHz (Figure 2a)	
assignment	N	I (%)	δ (ppm)	I (%)	δ (ppm)	I (%)	(Figure 2c) δ (ppm)	(Figure 2b) δ (ppm)	δ (ppm)	I (%)[a]
$R_2NCH_2C\mathbf{H}_3$	3	11.1	1.08	11.4	0.54	10.9	0.6	1.2	1.3	18.0
aryl-C$\mathbf{H}_3$	12	44.4	2.15	45.6	1.71	43.5	1.6			
$R_2NC\mathbf{H}_2CH_3$	2	7.4	2.56	7.2	2.06	7.6	(2.2)	2.7	1.9	58.2
$R_2NC\mathbf{H}_2$aryl	4	14.8	3.63	14.6	3.10	14.0	3.1	(3.3)		
aryl-**H**(1)	2	7.4	6.80	7.4	6.24	16.9	6.2	5.3[b]	5.4[b]	15.2
aryl-**H**(2)	2	7.4	6.85	7.4				6.3[b]	6.5[b]	
aryl-O**H**	2	7.4			7.58	7.2	8.4	8.2	8.1	5.1
$R_2N^+\mathbf{H}CH_2CH_3$							13.8		13.2	3.5

[a] The intensities for the MAS spectrum (Figure 2a) were obtained by a fitting procedure, the error of which is estimated to be ±10%. [b] In the solid state, the observation of two aromatic resonances is of different origin to that in the solution state, being a consequence of the packing arrangement discussed in the text.

sharp peak at 7.58 ppm corresponding to the hydroxyl proton, since, in the absence of a solvent, fast exchange does not occur. The line widths are clearly narrower in the liquid state, with the two aromatic protons only being partially resolved in Figure 2d, indicating that at the temperature used a low viscosity melt has not yet been reached.

We consider now the spectra of the solid dimer, starting with a discussion of the features which are evident from the simple MAS spectrum in Figure 2a. Although, even at a spinning frequency of 35 kHz, significant dipolar line broadening remains, four resonances at 1.3, 6.5, 8.1, and 13.2 ppm can be clearly distinguished, with shoulders at 5.4 and 1.9 ppm indicating two more. By analogy to the melt spectrum and by consideration of the fitted intensities, the fitted peaks at 1.3 and 1.9 ppm and those at 5.4 and 6.5 ppm can be assigned to all the alkyl and aromatic protons, respectively. This leaves two resonances at 8.1 and 13.2 ppm. On the basis of the proposed hydrogen-bonding scheme in Figure 1b, we expect the two formally hydroxyl protons per dimer (Figure 1a) to be distinct O−H and N−H hydrogen-bonded protons. In this case, the relative intensity of both peaks should be 3.7% each. Considering the fitted intensities in Table 1, the discrepancy for the peak at 8.1 ppm (5.1% rather than the expected 3.7%) is within the error inherent to the fitting of overlapping peaks.

In the melt, there is only one hydroxyl peak at 7.58 ppm (the intensity of 7.2% is in good agreement with the expected value of 7.4%). It is, therefore, informative to examine the changes in the spectrum upon both heating and cooling. In Figure 3, the change in the relative intensity of the resolved low-field hydrogen-bonded peak (at 13.2 ppm) as a function of temperature is plotted, together with the low-field region of the MAS spectrum at selected temperatures (for increasing temperature). It is then evident, as the sample melts, that the intensities of the two broad hydrogen-bonded peaks collapse to zero, while the intensity of the sharp peak grows from nothing. This behavior, together with the presence of only one peak at a moderate ppm value in the melt, indicates the presence, on the NMR time scale, of only free hydroxyl groups in the melt. A further consideration of Figure 3 shows a clear hysteresis between heating and cooling, and it should also be noted that slight changes in the NMR spectrum were observed upon recrystallization (for example, compare the MAS spectrum in Figure 2a—recorded after melting—to those shown later in Figures 4 and 5—recorded before melting).

In a previous study,[23] IR spectra of the methyl dimer in both the crystalline and molten states were obtained, and significant changes in the region corresponding to the hydrogen-bonded

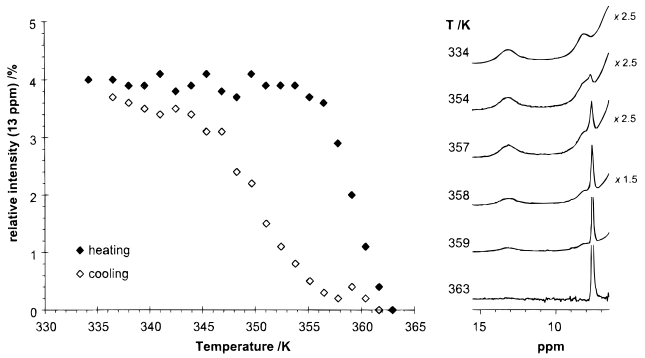

Figure 3. The effect of temperature on the low-field resonances of the ^{1}H MAS (at $\nu_R = 35$ kHz) NMR spectrum of the ethyl dimer upon heating and cooling. The plot (on the left-hand side) indicates the change in the relative integrated intensity of the resonance at 13.2 ppm as a function of the temperature. On the right-hand side, the change in the low-field region of the MAS spectrum upon heating is shown for selected temperatures.

protons were observed upon melting. In the spectrum of the molten sample, in addition to a peak at 3614 cm^{-1} that was assigned to free hydroxyl groups, a broad feature between 3100 and 3500 cm^{-1} was rationalized in terms of hydrogen bonding involving the nitrogen. A ^{1}H MAS NMR study (spectra not shown) of the melting of the methyl dimer produced analogous results to those obtained for the ethyl dimer, namely there was only evidence for free hydroxyl protons in the melt. The reasons for this apparent disagreement between the NMR and IR results are not clear. Possible explanations are the very different time scale of IR spectroscopy and the strong dependence of IR intensities on the transition dipole moments, such that the technique significantly discriminates in favor of hydrogen-bonded rather than free hydroxyl protons.

As mentioned in the Introduction, in recent years there has been major progress in the area of fast MAS, with the spinning frequency of 35 kHz only becoming commercially available in 1997. Such advances are particularly important for ^{1}H NMR of rigid solids. This is clearly illustrated in Figure 4, which presents ^{1}H MAS spectra of the ethyl dimer at spinning frequencies of 10, 15, 20, 25, 30, and 35 kHz. (The increase in intensity with increasing spinning frequency is due to the change in the ratio of the centerband to total intensity, with less signal being "lost" in spinning sidebands.) It should be noted that at 15 kHz, which until recently was the typical upper limit, only two peaks and two shoulders can be resolved, compared to the four peaks and two shoulders at 35 kHz.

Although at 35 kHz the resolution is much better than that at 15 kHz, it is clear that a true fast-spinning limit, which can be

(39) Wasylishen, R. E.; Fyfe, C. A. *Annu. Rep. NMR Spectrosc.* **1982**, *12*, 1.

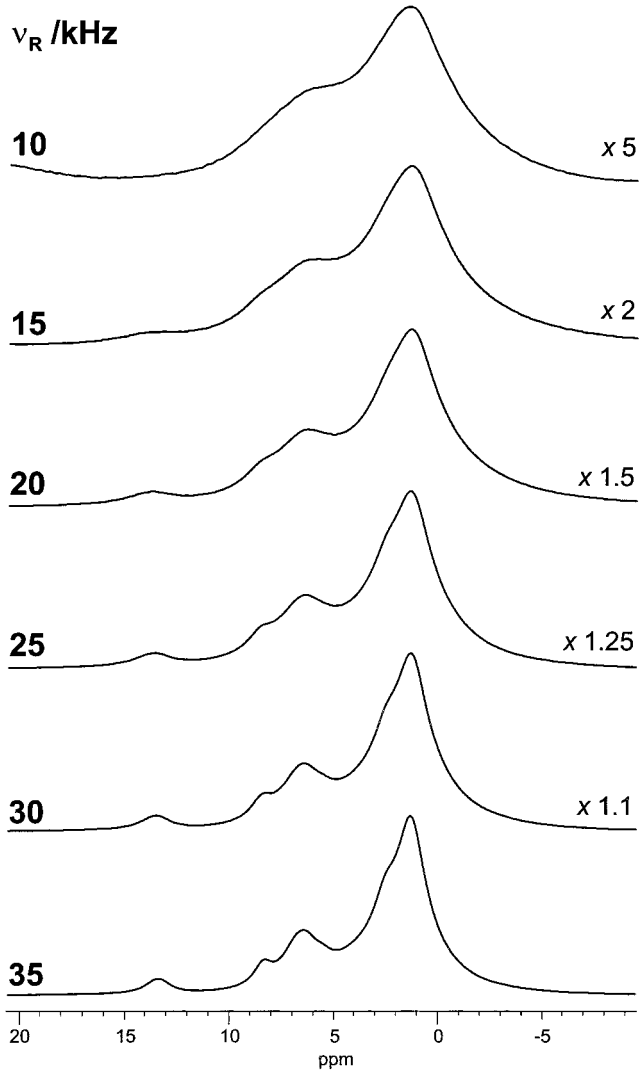

Figure 4. ^{1}H MAS NMR spectra of the ethyl dimer at different ν_R.

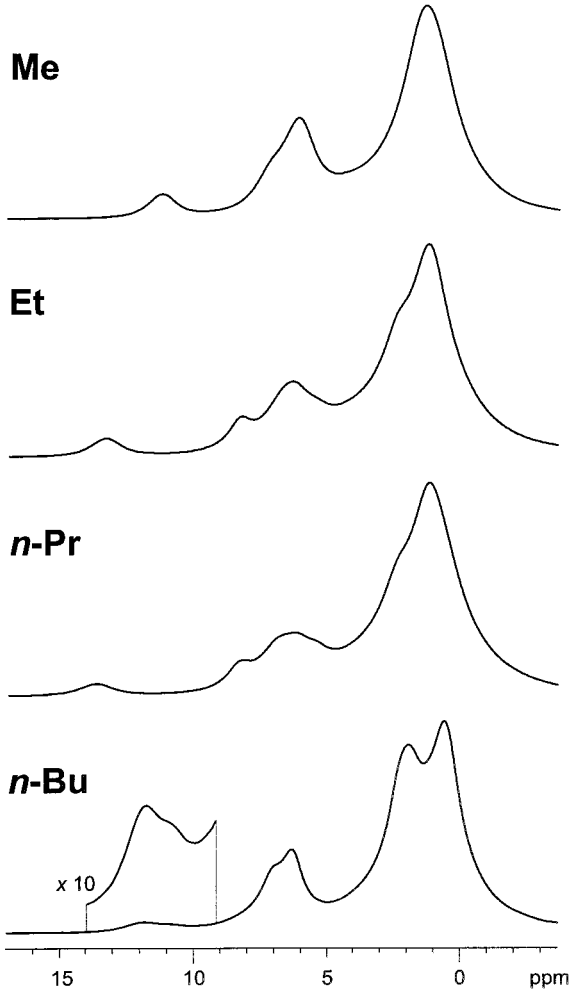

Figure 5. ^{1}H MAS NMR spectra of the four dimers at 35 kHz.

defined as the case where a further increase in ν_R does not result in further line narrowing, is still a long way off. Moreover, it is known, for a range of samples, that the CRAMPS technique can deliver significant enhancements in resolution compared to that observed in Figure 2a. In conventional CRAMPS experiments,[25] a low ν_R (typically 2−3 kHz) is used such that the sample can be considered to be quasi-static during the application of the multiple-pulse cycle, thus avoiding any destructive interference between the two simultaneous averaging processes. In this way, MAS is solely intended to remove the CSA, while the removal of the homonuclear dipolar broadening is left to the multiple-pulse cycle, and hence sequences designed to remove higher-order contributions to the average Hamiltonian (e.g. BR-24)[40] are used.

Recently, CRAMPS experiments requiring no special setup procedure, using the semi-windowless form of the simple WHH-4 sequence at rotation frequencies of 13−15 kHz, have been demonstrated to provide comparable resolution to that achievable by conventional CRAMPS on a model sample, namely L-alanine.[28] It was shown, for the synchronization condition $\tau_R/t_c = n$, where n is an integer greater than or equal to 3, that destructive interference is avoided, with the zero-order average Hamiltonian being completely reduced to zero at the end of each rotor period. The principle of this approach is different in that now MAS plays a role in the averaging of the homonuclear dipolar broadening. In this way, fast MAS can be thought of as taking care of the higher-order correction terms such that a shorter multiple-pulse method suffices.

Figure 2b presents the CRAMPS spectrum of the ethyl dimer, recorded with the semi-windowless WHH-4 sequence at 13 kHz, with $\tau_R/t_c = 6$. (As is usual for WHH-4 decoupling, the isotropic chemical shifts were observed to be scaled by 0.6, and hence the frequency axis was enlarged appropriately, such that the positions of the peaks are consistent with the other spectra.) For this CRAMPS experiment, it should be noted that the use of a semi-windowless WHH-4 sequence ($t_c = 12$ μs) means that the quasi-static limit is, to a first approximation, still achieved. At a spinning frequency of 35 kHz, however, such quasi-static conditions, and even the previously stated minimum synchronization condition of $\tau_R/t_c = 3$, become difficult to achieve. The fast-MAS approach is still nevertheless applicable, since it was found that another suitable synchronization condition is $\tau_R/t_c = 2/3$. In this way, the use of a semi-windowless pulse sequence is also avoided. The spectrum recorded at 35 kHz with a standard WHH-4 sequence with this synchronization condition is presented in Figure 2c (in this case, the isotropic chemical shifts were also found to be scaled by 0.6).

Comparing Figures 2a, 2b, and 2c, it is clear that significantly greater resolution is achieved for the CRAMPS experiments as compared to simple MAS, with the best resolution in Figure 2c for the CRAMPS experiment at 35 kHz. It is, however, also clear that the CRAMPS spectra are significantly noisier (no

(40) Burum, D. P.; Rhim, W.-K. *J. Chem. Phys.* **1979**, *71*, 944.

weighting functions were applied to the spectra in Figures 2b and 2c), and it should further be noted that it was found necessary, as a consequence of pulse breakthrough, to apply a large baseline correction to achieve acceptable spectra. Two important questions must then be asked: first, can we be sure that the observed peaks are genuine rather than artifacts; and second, are all the peaks which we expect to observe evident?

Consider first the low-field region of the spectra. While the peak at 8.1−8.3 ppm is clearly observed in all three spectra, this is not the case for the peak at 13.2 ppm, which is only clearly present in the simple MAS spectrum (Figure 2a). Except for a hint of a peak in Figure 2c, it is not evident above the noise level in the CRAMPS spectra. Lost intensity for protons dipolar coupled to ^{14}N, the latter being a quadrupolar nucleus (spin $I = 1$), has been observed in previous CRAMPS spectra,[41] and hence the missing peak in Figures 2b and 2c can be explained by assigning the resonance to the N−H protons. In this way, the CRAMPS spectra provide evidence for the presence of formal N−H bonds.

The improvement in resolution is most obvious in the alkyl region. A comparison of the CRAMPS spectrum at 35 kHz (Figure 2c) and the melt spectrum (Figure 2d) reveals that the reduction of the residual homonuclear broadening to the order of 1 ppm means that three of the alkyl peaks (at 0.6, 1.6, and 3.1 ppm) are clearly resolved in Figure 2c, with the shoulder at 2.1 ppm indicating the fourth. The resolution is less impressive in Figure 2b, and additionally a shoulder at 4.5 ppm has no equivalent in the simple MAS spectra of both the solid and melt samples, and must be an artifact.

Focusing on the aromatic region, both the simple MAS spectrum (Figure 2a) and the CRAMPS spectrum at 13 kHz (Figure 2b) show a second peak at 5.3 ppm, which has no obvious counterpart in either the melt or solution spectrum. This peak is not apparent in Figure 2c; however, this may be a consequence of the baseline distortion, since there is an obvious trough where the peak would be expected. The peak is clearly present as a shoulder in the MAS spectrum and, hence, cannot be simply an artifact of the multiple-pulse method. Instead, we hypothesize that we are observing two distinct aromatic peaks in the solid state which arise as a consequence of the packing arrangement of the dimers, as elucidated below in the discussion of the DQ MAS spectra. It is important to note that this is a different distinction to the observation of two aromatic peaks in the liquid, since the splitting observed in the solid (1 ppm) is much greater than that known from the liquid (0.05 ppm), such that the latter will certainly be lost under the residual dipolar broadening in the solid state. Instead, we mean that the molecular arrangement of the ethyl dimer induced by the proposed hydrogen-bonding scheme gives rise to a modified chemical shift of one of the four aromatic protons. It should be noted that, as a consequence of the inherent error of the fitting of the MAS spectrum (Figure 2a), it was, however, not possible to determine conclusively the number of protons corresponding to each resonance, and thus, in Table 1, the intensity due to the two types of aromatic protons has been grouped together.

A Comparison of the Four Dimers. Figure 5 compares the MAS spectra of the four different alkyl-substituted dimers. As discussed earlier for the ethyl spectrum in Figure 2a, two low-field resonances corresponding to the two distinct hydrogen-bonded protons can again be observed in the methyl and *n*-propyl spectra, while in the *n*-butyl spectrum, three resonances due to hydrogen-bonded protons can be distinguished, with the broad low-field peak corresponding to two distinct resonances (with fitted intensities in the ratio of 8 to 5). Table 2 lists the isotropic shifts of the hydrogen-bonded protons; a marked increase from methyl to ethyl and an equally marked decrease from *n*-propyl to *n*-butyl can be observed. It is further interesting to note that the two aromatic peaks, discussed above for the ethyl spectrum, are only apparent for the ethyl and *n*-propyl dimers. An additional difference between the spectra is in the high-field region corresponding to CH_2 and CH_3 protons; the observed changes here, however, are unsurprising considering the change in the nature of the *N*-alkyl chain.

Table 2. A Comparison of the Chemical Shifts of the Hydrogen-Bonded Protons

	δ (ppm)	
dimer	NH	OH
methyl	11.2	7.2
ethyl	13.2	8.2
n-propyl	13.6	8.2
n-butyl	12.0, 10.8	7.0

We first consider the assignment of the peaks corresponding to the hydrogen-bonded protons. In the discussion of the CRAMPS spectra of the ethyl dimer, the disappearance of the resonance at 13.2 ppm was explained in terms of the effect of dipolar coupling to nitrogen. Further evidence for such an assignment comes from the previous X-ray single-crystal study of the methyl dimer, which gave an O···O hydrogen-bonding distance of 0.29 nm. For a range of samples containing O−H···O hydrogen bonds, Berglund and Vaughan[9] and Harris *et al.*[11] have shown a correlation between the O···O distance and the ^{1}H isotropic chemical shift. From these studies, a value of 0.29 nm is more likely to be consistent with the observed shoulder at 7.2 ppm rather than the peak at 11.2 ppm in the methyl spectrum in Figure 5. Additionally, we note that similarly low-field shifted resonances have been previously observed for, for example, hydrogen-bonded N−H protons of Watson−Crick base pairs in yeast transfer RNA.[42] For the *n*-butyl dimer, the presence of a third hydrogen-bonding resonance indicates a more complicated packing arrangement as compared to the other dimers, which can be rationalized in terms of the increased steric competition between the benzene rings and the alkyl chain, as the latter becomes longer.

The studies by Berglund and Vaughan,[9] Jeffrey and Yeon,[10] and Harris et al.[11] of samples containing O−H···O hydrogen bonds have shown that an increase in the ^{1}H isotropic chemical shift corresponds to decreases in both the O···O and O···H distances. Since the latter are measures of the strength of the hydrogen bond, the ^{1}H isotropic chemical shift is hence also a direct indicator of the strength of the hydrogen bond. However, in this case, some care must be exercised since the previous studies have shown that a change of 2 ppm in the resonance frequency corresponds to, at the very most, a change of only 0.01 nm in the bond distance.

At first sight, an explanation for the observed trend in the chemical shifts of the hydrogen-bonded resonances could be hypothesized in terms of the interplay between the changing electronic and steric effects of the *N*-alkyl groups. With increasing chain length, a point will be reached where the steric bulk of the alkyl chain hinders the approach of the dimers forming the extended inter- and intramolecular hydrogen-bonded link. In this way, comparing the ethyl and *n*-propyl dimers with the *n*-butyl dimer, the observed shift of the hydrogen-bonded

(41) Naito, A.; Root, A.; McDowell, C. A. *J. Phys. Chem.* **1991**, *95*, 3578.

(42) Wüthrich, K. *NMR of Proteins and Nucleic Acids*; Wiley: New York, 1986; p 35.

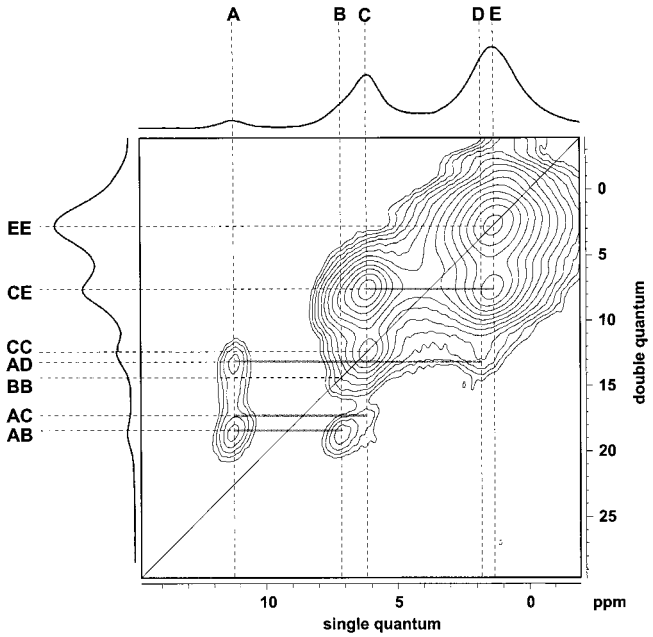

Figure 6. A rotor-synchronized ^{1}H DQ MAS NMR spectrum, together with skyline SQ and DQ projections, of the methyl dimer, recorded at 35 kHz with one cycle of the BABA recoupling sequence for the excitation and reconversion of DQC. The assignment of the peaks is discussed in the text.

resonances to high field could be understood. However, when comparing the methyl dimer with the ethyl and *n*-propyl dimer, the change of a single substituent from methyl to ethyl and *n*-propyl would not be expected to change the affinity of the amine nitrogen to protons to the extent that would be necessary to explain a 2 ppm low-field shift of the N−H···O resonance. Instead, lengthening the *N*-alkyl chain seems to induce a more profound change in the arrangement of the hydrogen bonds, which is accompanied by both a significant chemical shift change and a splitting of the aromatic proton resonances as has been pointed out above.

Two-Dimensional DQ MAS Spectra

In the previous sections, it has been shown that *one-dimensional* simple MAS and CRAMPS spectra can provide valuable information about the hydrogen-bonding arrangement in the benzoxazine dimers. A common approach in NMR is the extension of the experiment to a *second time dimension*; the correlation of the evolution frequencies in a two-dimensional spectrum then offers further new information about, for example, the proximity or connectivity of different nuclei. An example of such a method that is applicable to dipolar-coupled protons in a solid sample is the DQ MAS experiment. In this section, we first outline the general features of this approach, before presenting two-dimensional DQ MAS spectra of the four dimers.

While fast MAS is essential for achieving resolution in the solid state, the reduction in the residual dipolar coupling means that the excitation and reconversion of DQCs involving dipolar-coupled nuclei becomes inefficient. The CRAMPS experiments described earlier used a multiple-pulse sequence to remove the dipolar coupling; the concept can, however, easily be applied in reverse to reintroduce the necessary dipolar coupling during the excitation and reconversion periods of the experiment. Of the number of recoupling methods[34] suitable for this purpose, the BABA sequence[31] was used.

The DQ MAS spectrum of the methyl dimer in Figure 6 illustrates the general features of a typical DQ MAS spectrum. In the DQ dimension, resonances are present at the sum of the single-quantum (SQ) frequencies of the two involved nuclei. While DQCs between protons with identical chemical shifts yield auto peaks along the ($\nu_{DQ} = 2\nu_{SQ}$) diagonal, the intensity due to a DQC between protons with different SQ chemical shifts is split, in the SQ dimension, between a pair of cross-peaks symmetrically arranged on either side of this diagonal. The intensity of each peak is proportional to both the number of proton pairs giving rise to the DQC and the efficiency of DQ excitation and reconversion, with the latter depending strongly on the strength of the dipolar coupling.

The semiquantitative interpretation of the DQ MAS spectra outlined below is based on the spin-pair approximation,[32,34] which means that the dipolar interaction is assumed to produce only two-spin and negligible higher-spin correlations. This approach can be expected to be valid, to a first approximation, for the short excitation times used here, i.e., where the product of the considered dipolar coupling and excitation time is less than about 0.5. By this approximation, the efficiency of DQ excitation is proportional to the square of the dipolar coupling and is thus inversely proportional to the internuclear proton distance, *r*, to the power of six. This distance is smallest for methylene and methyl groups, and, additionally given their strong intensity in the one-dimensional spectrum, it is not surprising that the two-dimensional spectrum is dominated by the strong alkyl peak (EE). However, in the context of obtaining structural information, we are more interested in the lower intensity peaks, which are (even at the 3% contour threshold) well above the noise level.

An inherent advantage of the DQ MAS experiment is that the r^{-6} dependence means that the observation of a peak above the contour threshold is indicative of an effective proton−proton distance in the narrow range of 0.18 to 0.30 nm. (In this context, the term "effective" takes into account the case where more than one proton pair corresponds to a particular signal and refers to the proton−proton distance in a single hypothetical proton pair that would give rise to the same observed intensity.) Thus, considerable information can be obtained by a simple examination of the spectrum without recourse to a full quantitative investigation.

The Methyl Dimer. We will now examine in detail the spectrum of the methyl dimer in Figure 6. In the SQ (skyline) projection, only three peaks and a shoulder can be distinguished, corresponding to the N−H···O (A), the O−H···O (B), the aromatic protons (C), and the alkyl protons (E). However, as discussed below from the position of the peaks in the two-dimensional spectrum, it is possible to differentiate an additional type of alkyl proton (D).

When examining a DQ MAS spectrum, a key question to ask is which DQCs are present, and often more interestingly, which are not. For example, an obvious feature in Figure 6 is the absence of an N−H···O (AA) auto peak. Further considering the well-resolved N−H···O protons (A), obvious cross-peaks can be seen to the O−H···O (AB) and alkyl (AD) protons. In addition, there is some evidence of a weaker cross-peak to the aromatic protons (AC), and also a shoulder at about 15 ppm in the DQ dimension. The lack of resolution between the O−H···O (B) and the aromatic (C) protons and among the alkyl protons hinders the interpretation of the remainder of the spectrum. Nevertheless, the aromatic (CC) and alkyl (EE) auto peaks and the aromatic-alkyl (CE) cross-peaks can be clearly seen.

The three-dimensional structure, as determined by the previous X-ray and IR study,[23] of a hydrogen-bonded pair of methyl

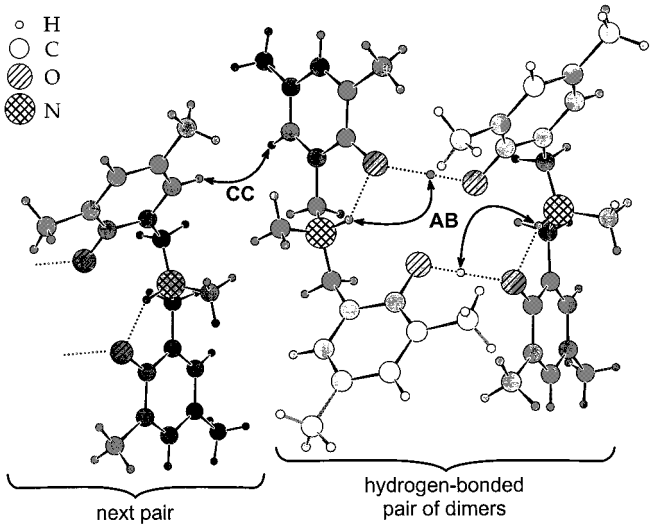

Figure 7. The three-dimensional structure, as determined by a previous single-crystal X-ray study,[23] of one hydrogen-bonded pair of methyl dimers and one dimer of a nearby pair. The positions of the formally hydroxyl protons were refined on the basis of both the previous IR[23] and this NMR study. The proposed extended hydrogen-bonded links are indicated by dotted lines. Additionally, the proximity of N−H···O and O−H···O protons, and two aromatic protons giving rise to the AB cross-peaks and a CC auto peak, respectively, in the observed DQ MAS spectrum are indicated. A sense of depth is indicated by the shading, with light spheres indicating atoms which are coming out of the page.

dimers, and one further nearby dimer is presented in Figure 7. For emphasis, the hydrogen-bonding arrangement and the intermolecular AB and CC pairs are also indicated. Table 3 then lists all proton pairs in the structure (per individual dimer) whose internuclear distances are less than or equal to 0.3 nm, i.e., all those that would be expected to give rise to peaks in the DQ spectrum. For many proton pairs, there is more than one pair of the same type per dimer, for example, consider the proton pairs corresponding to the EE cross-peak, i.e., those between *Ar*-CH_3 protons. There are four distinct methyl groups each with three distinct intra-group proton pairs with the same internuclear distance (0.18 nm); this is indicated in Table 3 by the notation 12×0.18. As a further example, consider proton pairs among the CH_2 protons. In each dimer, there are two such methylene groups. There are therefore two intra-group pairs (as indicated by 2×0.18) as well as four inter-group pairs with proton−proton distances of 0.22, 0.26, 0.28, and 0.29 nm.

Most proton−proton distances in Table 3 were calculated with use of the proton positions given in ref 23 (as determined from the X-ray diffraction pattern). However, the exact localization of protons in a structure with use of single-crystal X-ray diffraction data is very difficult, since the scattering is proportional to the electron density of an atom and hence is weakest for protons,[44] and instead the computer programs used to interpret X-ray data often position the protons based on the well-established knowledge of the geometries for different hydrogen-containing moieties. As an example of the errors inherent to the determination of proton positions in this way, the program used by Dunkers et al.[23] gave unrealistic positions for the hydrogen-bonded "hydroxyl" protons. Instead the alternative "hydroxyl" proton positions shown in Figure 7, and from which the distances in Table 3 were calculated, were determined on the basis of the IR[23] and this NMR study as well as a knowledge of other hydrogen-bonded structures[45] in the literature. In addition, the values for the proton−proton distances within the CH_2 and CH_3 groups given in Table 3 are those determined by previous NMR[32,46] and neutron diffraction[47] studies rather than the unrealistically short values (0.15 nm) based on the positions in ref 23. Additionally, it should be noted that, to take into account the fast rotation of the methyl protons, the distances to these protons, given in Table 1, are measured to the respective carbon atoms. In any quantitative analysis, the reduction, due to this fast rotation, of the dipolar coupling must be taken into account. In particular, the *intra*-methyl interaction is reduced by a factor of 0.5, and the coupling to protons external to the group is scaled by a factor between 0.5 and 1, depending on the orientation of the internuclear vector with respect to the methyl rotation axis.[48,49]

We will now rationalize the observed spectrum in terms of the proton−proton distances in Table 3, considering first the N−H···O protons (A). As shown in both Figures 1b and 7, the packing of the dimers in the solid-state structure is strongly influenced by the intramolecular N−H···O and intermolecular O−H···O hydrogen bonds which together form an extended N−H···O···H−O link. The two protons of these double hydrogen bonds give rise to the two cross-peaks at (A, AB) and (B, AB). (The notation (X, Y) indicates a two-dimensional peak centered at SQ and DQ frequencies of X and Y, respectively.) There will be one more (N−H···O) (O−H···O) pair within a pair of dimers, involving protons from the two distinct hydrogen-bonded links. However, from the proposed structure this proton−proton distance is predicted to be significantly greater than that for the closest pair (0.35 nm compared to 0.27 nm), and hence the contribution of this pair to the observed intensity is expected to be negligible. The proposed structure further predicts the nearest distance between two N−H···O protons to be 0.55 nm, thus explaining the absence of an AA auto peak.

As expected from Table 3, a cross-peak (AD) to the *N*-methyl protons is clearly evident in Figure 6. The position of the center of this peak corresponds to a SQ frequency (D) slightly shifted from the maximum in the SQ projection. This is not surprising since there are both *N*- and *Ar*-methyl groups, which are likely to give rise to proton resonances with different chemical shifts. At MAS frequencies of 35 kHz, these two shifts are not resolved. There are four times more *Ar*-methyl groups per dimer, and hence the auto peak (EE) would be expected to be centered at the *Ar*-methyl chemical shift. From Table 3, the N−H···O protons are not close to the *Ar*-methyl protons, and thus a cross-peak is only expected to the *N*-methyl protons; the presence of a shoulder at (D, AD) rather than (E, AE) and the centering of peak at (A, AD) rather than (A, AE) support this.

Again from Table 3, the N−H···O protons are expected to be close to the four methylene protons. On the basis of the CRAMPS spectra of the solid ethyl dimer and also the melt and solution-state spectra in Figure 2, it is expected that these CH_2 protons would have a chemical shift in the region of 3 ppm. There is, however, no evidence of the expected cross-peak to the N−H···O protons at (3 ppm, A + 3 ppm) and only a weak shoulder at (A, A + 3 ppm). A further discrepancy between the observed spectrum and the proposed structure is

(43) Bennett, A. E.; Griffin, R. G.; Vega S. *NMR* **1994**, *33*, 1.
(44) McKie, D.; McKie, C. *Essentials of crystallography*; Blackwell: Oxford, 1986; Chapter 9.
(45) Zeegers-Huyskens, T. *Spectrochim. Acta* **1965**, *21*, 221.
(46) Andrew, E. R.; Bersohn, R. *J. Chem. Phys.* **1950**, *18*, 159.
(47) Delaplane, R. G.; David, W. I. F.; Ibberson, R. M.; Wilson, C. C. *Chem. Phys. Lett.* **1993**, *201*, 75.
(48) Sekine, S.; Kubo, A.; Sano, H. *Chem. Phys. Lett.* **1990**, *171*, 155.
(49) Friedrich, U.; Schnell, I.; Demco, D. E.; Spiess, H. W. *Chem. Phys. Lett.* **1998**, *285*, 49.

Table 3. Internuclear Distances (nm) of Proton Pairs in the Methyl Dimer Based on the X-ray Structure Analysis[23]

					CH arom[d]			
		Ar-CH_3[a]	*N*-CH_3[a]	CH_2	ortho	para	OH[e]	NH[f]
		E	D		C		B	A
Ar-CH_3[a]	E	12 × 0.18[b]			6 × 0.27	12 × 0.27	3 × 0.28	
N-CH_3[a]	D		3 × 0.18[b]	6 × 0.26				3 × 0.20
CH_2			6 × 0.26	2 × 0.18[c]	2 × 0.24	0.28		2 × 0.24
				0.22				2 × 0.29
				0.26				
				0.28				
				0.29				
CH arom[d] *ortho*	C	6 × 0.27		2 × 0.24	*0.27*			
para		12 × 0.27		0.28		*0.30*		
OH[e]	B	3 × 0.28					0.29	0.27
NH[f]	A		3 × 0.20	2 × 0.24			0.27	
				2 × 0.29				

[a] For DQCs involving protons external to the CH_3 group, carbon positions are used instead of proton positions because of the effect of fast methyl rotation. [b] Intra-methyl proton−proton distance known from NMR experiments.[46] [c] Intra-methylene proton−proton distance known from NMR experiments[32] and neutron diffraction.[47] [d] *Ortho* and *para* positions are given relative to the (−CH_2−NR−CH_2−) bridge. [e] Proton position derived from DQ NMR spectra. [f] Proton bonded to nitrogen as proposed in Figure 5 of ref 23 and as confirmed by this NMR study.

the presence of signal, albeit of weak intensity, at (C, AC) indicative of aromatic protons which are close to N−H···O protons. However, according to the proposed structure, the closest such inter-proton distances are far too large (over 0.4 nm) to explain the observed intensity. We will return to these points later.

For the O−H···O protons (B), only one distinct DQC is clearly evident, namely the cross-peak (AB) to the N−H···O protons. However, from Table 3, both the *Ar*-methyl protons and the O−H···O proton of the other hydrogen-bonded link are sufficiently close to expect, albeit weak, BE cross-peaks and a BB auto peak. In both cases, the presence of nearby (CE and CC) strong intensity which could easily obscure these peaks means, however, that care should be exercised in the interpretation of these parts of the spectrum. Indeed, there does appear to be a shoulder where the BB auto peak is expected.

Looking at the aromatic protons (C), the intense CE cross-peak to the *Ar*-methyl protons is clear. More interesting, though, is the CC auto peak. The distance between the two protons on a single benzene ring is too large (0.40 nm) to explain the observed intensity. Instead, as indicated in Figure 7 and by the italics in Table 3, the peak is due to intermolecular pairs of aromatic protons on dimers which do not form a hydrogen-bonded pair. For each dimer, there are two aromatic protons which form such pairs, namely an *ortho* proton of one ring (which is close to another *ortho* proton) and a *para* proton of the other ring (which is close to another *para* proton on a different dimer), with the internuclear distance being shorter in the former case (only the former case is shown in Figure 7).

In conclusion, the principal features of the DQ spectrum are in agreement with the proton−proton proximities in Table 3, and thus confirm the refined X-ray structure from which the proton−proton distances were calculated.

The Ethyl Dimer. The two-dimensional DQ MAS spectrum of the ethyl dimer is shown in Figure 8. Although similar to that of the methyl dimer, there exist some profound differences. Among the alkyl protons, residual homogeneous broadening means that only two peaks (D) and (E) can be identified, and thus it is not possible to differentiate between DQCs due to the *Ar*- and ethyl-chain methyl protons. Nevertheless, many important features are still apparent. As for the methyl spectrum, clear AB cross-peaks between the N−H···O and O−H···O protons can be identified, thus providing evidence for the same type of extended N−H···O···H−O hydrogen-bonded link in both samples.

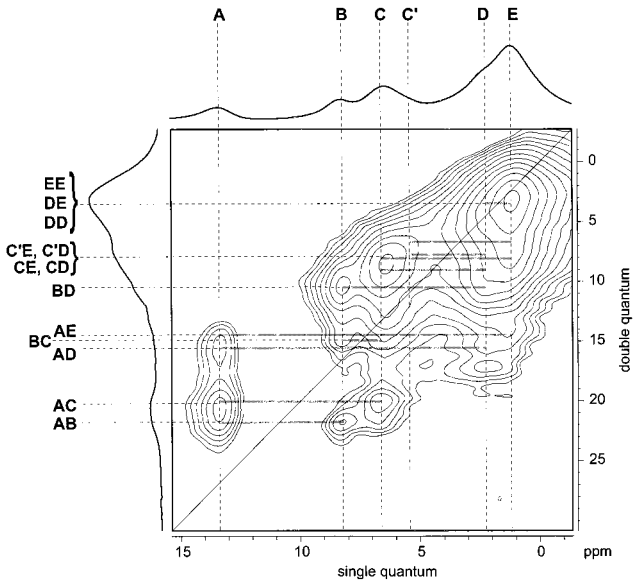

Figure 8. A rotor-synchronized ^{1}H DQ MAS NMR spectrum, together with skyline SQ and DQ projections, of the ethyl dimer, recorded at 35 kHz with one cycle of the BABA recoupling sequence for the excitation and reconversion of DQC. The assignment of the peaks is discussed in the text.

The most striking differences between the methyl- and ethyl-dimer spectra are that while for the methyl dimer there is a strong aromatic auto peak (CC) and only weak intensity corresponding to a DQC between a N−H···O and an aromatic proton (AC), the situation is reversed for the ethyl dimer. As discussed above, the strong aromatic auto peak in the methyl dimer is due to the close proximity of two aromatic protons of two different hydrogen-bonded dimer pairs, and the clear difference in the ethyl spectrum therefore indicates an alternative packing arrangement.

A consideration of the basic structure of the benzoxazine dimer reveals that the observation of both the strong AC peak and the absence of the CC peak for the ethyl dimer can be explained if one of the aromatic rings is flipped such that instead of pairs of hydrogen-bonded dimers there exist hydrogen-bonded chains as shown in Figure 9. In addition, this alternative packing arrangement gives rise to a close proximity of the O−H···O proton and the *N*-ethyl chain. The resulting cross-peak between the O−H···O proton and the ethyl-chain CH_2 protons (BD) is, indeed, clearly seen in the DQ MAS spectrum of the ethyl dimer.

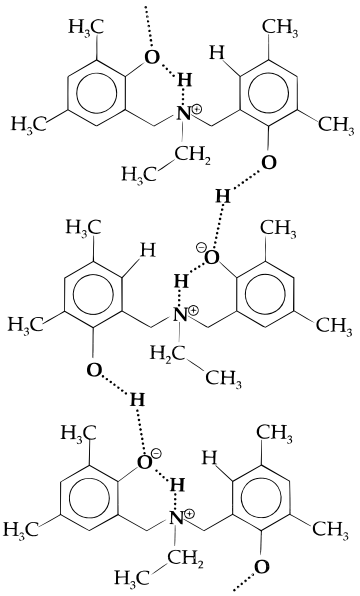

Figure 9. A schematic representation of an alternative linear arrangement of hydrogen-bonding dimers, which can be used to explain the principal features of the DQ MAS spectrum of the ethyl dimer.

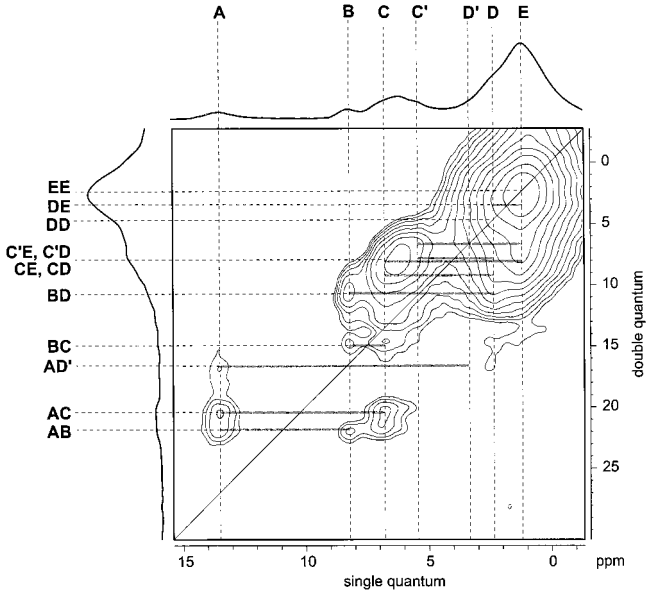

Figure 10. A rotor-synchronized ^{1}H DQ MAS NMR spectrum, together with skyline SQ and DQ projections, of the *n*-propyl dimer, recorded at 35 kHz with one cycle of the BABA recoupling sequence for the excitation and reconversion of DQC. The assignment of the peaks is discussed in the text.

For the methyl dimer, where pairs of hydrogen-bonded dimers are believed to form, an analogous peak between the O−H···O proton and the *N*-methyl protons is neither predicted by the crystal structure nor apparent in the DQ spectrum in Figure 6. Moreover, the presence and the intensity of an additional aromatic proton resonance (C′) for the ethyl dimer seems to further support this alternative arrangement.

The *n*-Propyl Dimer. An examination of the DQ MAS spectrum of the *n*-propyl dimer in Figure 10 reveals close similarities to that of the ethyl dimer in Figure 8. In both spectra, cross-peaks can be identified between the N−H···O proton and the O−H···O proton (AB), and one type of aromatic proton (AC), as well as between the O−H···O proton and one type of aromatic proton (BC), and the alkyl-chain CH_2 protons (BD). The fact that the intensities of the DQCs involving A and B protons are less for the *n*-propyl dimer than compared to the ethyl dimer indicates that the proton−proton distances among the N−H···O···H−O hydrogen bonds are slightly greater in the *n*-propyl dimer; this is probably caused by the steric demands of the longer *N*-alkyl chain.

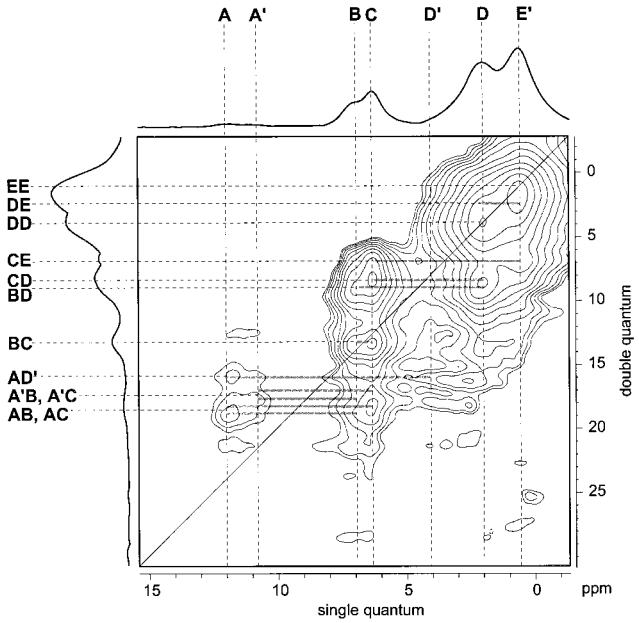

Figure 11. A rotor-synchronized ^{1}H DQ MAS NMR spectrum, together with skyline SQ and DQ projections, of the *n*-butyl dimer, recorded at 35 kHz with one cycle of the BABA recoupling sequence for the excitation and reconversion of DQC. The assignment of the peaks is discussed in the text.

One small difference involves the cross-peak between the N−H···O proton and the alkyl protons; for the ethyl dimer, a strong cross-peak (AD) is seen to *N*-CH_2 protons, while for the *n*-propyl dimer, only a weak cross-peak to the alkyl protons is evident, which seems to involve the CH_2 protons between the aromatic ring and the nitrogen (AD′) more strongly than the *n*-propyl protons. However, the absence of intensity at (D′, AD′) in the *n*-propyl spectrum means that care must be taken with the interpretation of cross-peaks to these CH_2 protons. Indeed, it appears a general feature of the DQ MAS spectra of all the dimers that peaks involving these CH_2 protons at their SQ frequency are either absent or of such weak intensity that they are indistinguishable from the tails of the other intense alkyl peaks. The origin of this effect is not clear, possibly being due to a combination of fast relaxation and the presence of spectral distortions in the tail region of the other strong alkyl peaks.

The *n*-Butyl Dimer. Finally, we consider the DQ MAS spectrum of the *n*-butyl dimer in Figure 11. As noted earlier in the discussion of the MAS spectrum in Figure 5, there are two N−H···O resonances (A and A′), and cross-peaks involving both are observed. In the alkyl region, only two peaks are resolved. From the observed chemical shifts, these would appear to correspond to the *N*-CH_2 and CH_3 (E′) protons of the *n*-butyl chain. However, the contribution of the resonances of the other three types of alkyl protons will be present in this region and hence an unambiguous interpretation of peaks to the alkyl protons is not possible. Additionally, for the *n*-butyl dimer, only one aromatic resonance (C) can be distinguished, and the O−H···O and aromatic peaks are less well separated as in Figures 8 and 10. Taking these considerations into account, the *n*-butyl spectrum is still similar to that of the ethyl and *n*-propyl dimers.

Table 4. A Comparison of the DQ MAS Spectra

	DQCs									
dimer	AB	AC	AD	AD′	AE	BC	BD	CC	CD	CE
methyl	+	(+)	+	?				+	(+)	+
ethyl	+	+	+	?	+	+	+	(+)	+	+
n-propyl	+	+	?	+	?	+	+	(+)	+	+
n-butyl	+	+	(+)	+	?	+	+	(+)	+	(+)

Although the cross-peaks at the SQ frequency of the N−H···O protons (A and A′) are at the same intensity of what appear to be spurious peaks at the tail of the alkyl region, as for the ethyl and *n*-propyl dimers but not for the methyl dimer, cross-peaks are evident between these N−H···O protons and both the O−H···O protons (AB and A′B) and the aromatic protons (AC and A′C), as well as between the O−H···O proton and both the aromatic protons (BC) and the alkyl-chain CH_2 protons (BD). The fact that, at the N−H···O resonance, a cross-peak between the N−H···O proton and the *Ar*-CH_2−NR protons (AD′) is more clearly present than that to the other alkyl protons is reminiscent of the *n*-propyl spectrum.

A Comparison of the Dimers. To permit an easier comparison of the DQ MAS spectra of the methyl, ethyl, *n*-propyl, and *n*-butyl dimers, Table 4 indicates which DQCs are observed in each spectrum (cross and auto peaks among the alkyl protons are not indicated). With regards to an understanding of the hydrogen bonding, two important features should be noted: first, cross-peaks between the N−H···O and O−H···O protons (AB) are observed in all spectra; and second, while the spectra of the ethyl, *n*-propyl, and *n*-butyl dimers are very similar, as a group they show significant differences to the spectrum of the methyl dimer. The following conclusions can therefore be drawn: the same extended inter- and intramolecular hydrogen-bonded link, N−H···O···H−O, appears to be present in all dimers, but while for the methyl dimer, pairs of hydrogen-bonded dimers are preferred, for the ethyl, *n*-propyl, and *n*-butyl dimers, a chain arrangement seems more likely.

In the DQ MAS spectrum of the methyl dimer in Figure 6, a cross-peak between N−H···O and aromatic protons (AC), although weak, is clearly present. As stated earlier, this cannot be explained by the proposed single-crystal X-ray structure. In light of the spectra of the other dimers, however, it can be explained by hypothesizing the presence of, in addition to simple pairs of hydrogen-bonded dimers, a minority amount of dimers linked in a linear arrangement. It is not surprising that the X-ray study did not identify such a minority phase, since the careful selection of a suitable single crystal would be likely to differentiate in favor of the majority component.

Conclusions and Summary

In this paper, fast-MAS NMR methods have been used to investigate hydrogen bonding in a series of benzoxazine dimers. First, simple MAS spectra, obtained at the only recently available spinning frequency of 35 kHz, clearly demonstrated that the two "formally" hydroxyl protons are not equivalent in the solid state, with strong hydrogen bonding being indicated by the pronounced low-field shift of one of the peaks. These observations are consistent with the existence of extended inter- and intramolecular hydrogen-bonded links between dimers, as proposed previously by Dunkers et al.[23]

A significant low-field shift of the chemical shifts of the hydrogen-bonded protons was observed on increasing the chain length from methyl to ethyl. Together with the observation of two distinct aromatic proton resonances in only the MAS spectra of the ethyl and *n*-propyl dimers, this suggests a different packing arrangement for the methyl and ethyl dimers. Additionally, the suitability of NMR to the study of temperature-dependent processes allowed an investigation of the changes which occur on melting, and it was observed that the extended hydrogen-bonding arrangement collapsed on melting, giving a single free hydroxyl resonance.

For the ethyl dimer, spectra obtained by using an alternative CRAMPS approach applicable at high spinning frequencies were presented. It was shown that significant resolution enhancements, similar to what would be expected for a conventional CRAMPS experiment, could be achieved. Importantly, unlike for a conventional CRAMPS experiment, no special sample preparation or experimental setup procedures were necessary. The resolution was particularly impressive for the CRAMPS experiment at 35 kHz, where the new synchronization condition of three multiple pulse cycles for every two rotor periods was used. Unlike the earlier demonstrations at 13−14 kHz, in this case, the sample can in no way be considered to be quasi-static during the application of the multiple-pulse sequence. Further work considering refinements of this new approach is underway and will be presented in due course.

The DQ MAS spectra of the four different dimers showed the value of extending the NMR experiment to a second dimension. For the methyl dimer, the proton proximities identified by the DQ MAS spectra support the presence of hydrogen-bonded pairs of dimers, as proposed in a previous X-ray and IR study. However, the clear differences between the methyl spectrum and the spectra of the other dimers could only be explained by proposing an alternative hydrogen-bonded chain arrangement for the latter case.

In a previous study, Ishida and Low[20] investigated the effect caused by altering the length of the alkyl chain substituent on the hydrogen-bonding arrangement in benzoxazine dimers by molecular modeling. They showed that a clear change occurred on going from methyl to ethyl. However, the constraints of the molecular modeling package meant that they could only consider the intramolecular hydrogen bonding that would occur within an isolated single dimer. As a consequence, the N−H distance was calculated to be between 0.204 and 0.207 nm; such values are clearly inconsistent with the convincing NMR evidence in this paper for the existence of formal N−H bonds (bond distance 0.10 nm). Additionally, the molecular modeling calculation considering only an isolated dimer was, of course, unable to identify the different intermolecular hydrogen-bonding arrangements elucidated by the DQ MAS spectra presented here.

The ability to extract such detailed information about the proximity of nearby protons in these rigid solids from the DQ MAS spectra is strongly dependent on the increased resolution achievable at 35 kHz. However, even at this very-fast spinning frequency, some overlapping peaks are not resolved. Recently, CRAMPS methods have been applied in both dimensions of a DQ MAS spectrum.[35] Although improved resolution was achieved, it was at the expense of the introduction of spurious signals. Moreover, we are especially interested in the peaks due to hydrogen-bonded protons on the nitrogen, which as stated above are not observed in the CRAMPS spectra. Therefore, in this study, no attempt to improve the resolution in the DQ MAS spectra by a CRAMPS approach was made. In this context, it is however interesting to note that the exact positions of the cross-peaks in the two-dimensional spectra, in some cases, permitted the resolution of distinct protons, which could not be resolved in the SQ projection.

In this paper, the DQ MAS spectra have been analyzed in only a semiquantitative manner. The wealth of information that

can be achieved by such a straightforward analysis illustrates an important advantage of the DQ MAS experiment, namely that the inverse dependence of the DQ excitation efficiency, to a first approximation, on the internuclear distance to the sixth power means that the mere observation of a peak indicates an effective internuclear distance of less than 0.3 nm. Moreover, directly quantitative information can, in principle, be obtained from these DQ MAS spectra for peaks for which the consideration of a DQC as arising from an isolated spin pair is applicable. As an example, Graf *et al.*[50] have recently presented an analysis of polymer chain order and dynamics in a polybutadiene melt based on the quantitative analysis of ^{1}H DQ MAS spectra. In the present study, one H−H internuclear distance of particular interest is that in the extended hydrogen-bonded link, N−H···O···H−O (i.e. in the notation of Table 3, that between the A and B protons). In a separate experiment, using the isolated H−H pair present in CBr_3COOH dimers as an external standard, this distance was determined to be 0.27 nm (see Table 3). A full discussion of the quantitative interpretation of DQ MAS spectra with such external standards will be presented elsewhere.

Although it can be hoped that future advances will further increase the information that can be obtained by ^{1}H MAS NMR methods, these methods alone will probably never be able to provide an unambiguous assignment of all protons in a structure. Therefore, it is important to consider how the approaches described in this paper fit into the context of other available techniques. The standard method for structure determination is X-ray single-crystal diffraction. However, as noted earlier, X-rays are scattered by electrons, and hence the exact localization of hydrogen atoms (the element with the lowest electron density) with X-rays is normally not possible. It is therefore often necessary to use information provided by other techniques to refine the structure; in this context the complimentary NMR methods are very useful.

As an alternative to X-ray analysis, neutron scattering[44] can be used. This latter method has the advantage that the scattering of neutrons is not biased against lighter elements. However, it turns out that protons are particularly badly suited to neutron scattering because of their large incoherent cross section. Instead, except for very simple molecules, it is necessary to deuterate the sample. The effort that would be required for such a synthesis, combined with the considerable expense of neutron scattering facilities, means that the technique is certainly not routinely used for the localization of hydrogen atoms in a structure. Additionally, it must be remembered that the bond lengths in a hydrogen bond would be slightly altered by substituting protons with deuterons.

In the past decade, a number of ingenious solid-state NMR methods have been presented which allow the accurate determination of internuclear distances, most notably the REDOR technique.[51] Additionally, by using a modified version of the standard DQ MAS experiment employed in this paper, even torsional angles have been determined.[52−56] However, one feature these methods have in common is the chemically demanding requirement for the introduction of two or more specific isotopic labels, such that isolated small spin systems are achieved. Moreover, the techniques are not applicable to determining proton−proton distances unless all but the two protons of interest could be deuterated.

This paper has shown that solid-state ^{1}H fast-MAS NMR methods at the commercially available spinning frequency of 35 kHz can deliver much information about systems of chemical interest. In particular, neither isotopic labeling nor the preparation of a single crystal were required. Furthermore, sensitivity is not a problem for ^{1}H NMR, and even the two-dimensional DQ MAS spectra could be obtained in 85 min (this experimental time is limited by the length of the phase cycle, rather than sensitivity).

In conclusion, the ease and speed with which information can be obtained by these ^{1}H fast-MAS NMR methods is an obvious advantage, and the insights provided can then be used to devise a strategy whereby other, more time-consuming, approaches can be pursued so as to build up a complete picture. In the present study of the benzoxazine dimers, one possible avenue for future work would be the synthesis of ^{15}N-labeled benzoxazine dimers; in this way, the N−H bond distance could be accurately determined by a heteronuclear ^{15}N−^{1}H DQ MAS experiment.

It is further hoped that an understanding of these model compounds can be extended to the polybenzoxazine systems. For example, it is interesting to note, in the context of the different packing arrangements of benzoxazine dimers elucidated in this study, that while the shrinkage or expansion on curing was less than 0.8% for ethyl, *n*-propyl, and *n*-butyl monomers, it was significantly greater (a shrinkage of +3.2%) for the methyl monomer.[20] Moreover, preliminary simple MAS and DQ MAS spectra have been obtained for a polybenzoxazine sample, which indicate the presence of related hydrogen-bonding arrangements to those observed in the model dimers.

Acknowledgment. Financial support from the Deutsche Forschungsgemeinschaft, SFB 262, is acknowledged. S.P.B. thanks the Alexander von Humboldt-Stiftung for the award of a research fellowship. H.Y.L. and H.I. gratefully acknowledge the financial support of the National Science Foundation Center for Molecular and Microstructure of Composites. We thank Dr. Manfred Wilhelm for stimulating discussions and Dr. Susan De Paul for carefully proof reading the manuscript.

JA982766T

(50) Graf, R.; Heuer, A.; Spiess, H. W. *Phys. Rev. Lett.* **1998**, *80*, 5738.
(51) Gullion, T.; Schaefer, J. *Adv. Magn. Reson.* **1989**, *13*, 57.
(52) Feng, X.; Lee, Y. K.; Sandstrøm, D.; Edén, M.; Maisel, H.; Sebald, A.; Levitt, M. H. *Chem. Phys. Lett.* **1996**, *257*, 314.
(53) Feng, X.; Verdegem, P. J. E.; Lee, Y. K.; Sandstrøm, D.; Edén, M.; Bovee-Geurts, P.; de Grip, W. J.; Lugtenburg, J.; de Groot, H. J. M.; Levitt, M. H. *J. Am. Chem. Soc.* **1997**, *119*, 6853.
(54) Feng, X.; Edén, M.; Brinkmann, A.; Luthman, H.; Eriksson, L.; Gräslund, A.; Antzutkin, O. N.; Levitt, M. H. *J. Am. Chem. Soc.* **1997**, *119*, 12006.
(55) Hong, M.; Gross, J. D.; Griffin, R. G. *J. Phys. Chem. B* **1997**, *101*, 5869.
(56) Costa, P. R.; Gross, J. D.; Hong, M.; Griffin, R. G. *Chem. Phys. Lett.* **1997**, *280*, 95.